

ppap.200731808C

Full Paper

The nitrogen chemical potential is shown to depend on the process temperature even if the same nitrogen flux is applied due to the diffusion of nitrogen to

the bulk. The nitrogen profile and surface chemical state also depend on the temperature showing that the formation of precipitates plays a major role.

Precipitates Temperature Dependence in Ion Beam Nitrided AISI H13 tool steel

L. F. Zagonel,* R. L. O. Basso, F. Alvarez

Plasma Process. Polym. **2007**, *4*, S1–S5



WILEY-VCH

Precipitates Temperature Dependence in Ion Beam Nitrided AISI H13 Tool Steel

Luiz F. Zagonel,* Rodrigo L. O. Basso, Fernando Alvarez

AISI H13 tool steel samples were nitrided using broad nitrogen ion beams in a high-vacuum chamber at different temperatures. At 400 °C, a thin ϵ -Fe₂₋₃N phase forms on the top of a shallow nitrided layer and the nitrogen distribution follows a complementary error function. At 500 °C, deviations from this behavior are observed and a thick ϵ -Fe₂₋₃N layer is formed. At 600 °C, no ϵ -Fe₂₋₃N phase is formed and the nitrogen profile is step-like. At such a temperature, coarse nitride precipitates are observed. Also, carbon losses (decarburizing) are observed upon nitriding at and above 500 °C.

Introduction

Nitriding is a well-established industrial surface treatment for improving mechanical, tribological, and corrosion resistance of metallic alloys such as tool steels.^[1,2] Plasma nitriding is of particular interest due to the precise control of the compound layer and diffusion layer properties, its versatility, and its environment friendliness.^[3] In this technique, ionized nitrogen species impinge the material surface with energies determined mainly by the applied voltage and the chamber gas pressure. The energy of the ionized species can be large enough as to cause them to break-up at the metallic surface and form free N which diffuses into the material.^[4,5] Depending on the material and process parameters, like ion current density and temperature, nitriding may induce the formation of precipitates and of iron nitride phases. In particular, a compact monolayer ϵ -Fe₂₋₃N is known to provide better corrosion resistance, wear endurance, and low surface friction.

The understanding of the nitriding process is important for its optimization. As it is well established, the formation of precipitates is one important cause of mechanical properties improvements in nitrided steels. We remark, however, that coarse precipitation can lead to undesired

results, like decreased corrosion resistance, and should be avoided. In this study, we report nitriding experiments performed using a low energy broad beam ion source in high-vacuum conditions at different temperatures and its influence on microstructural material properties. At 400 °C, very high nitrogen surface concentration and nanometric precipitates are obtained. At higher temperature (600 °C), the nitrogen surface concentration is reduced by fast diffusion into the material and desorption. Finally, at this relatively high temperature, microscopic precipitates are formed.

Experimental Part

Rectangular samples (2 × 15 × 20 mm³) were cut from a single tempered AISI-H13 lot (7.5 ± 0.4 GPa bulk hardness). Table 1 displays the material composition as determined by the chemical analysis by means of inductive-coupled plasma-optic emission spectroscopy. The slices were polished up to 1 μm diamond paste and cleaned in an acetone ultrasonic bath. The final surface roughness was 40 nm (R_a), as measured by profilometry. One at a time, the samples were introduced into the ion beam nitriding chamber (base pressure <10⁻⁵ Pa) attached to an ultra-high vacuum in situ X-ray photoemission spectroscopy (XPS). The ion beam source is a broad beam Kaufman cell, adjusted to 400 eV and 1.5 mA · cm⁻² for all the samples.^[6] The sample temperature is controlled by a thermocouple in contact with the heating sample holder and the ion current density determined by means of a Faraday cup. More experimental details of the system can be found elsewhere.^[7] The samples were nitrided for 300 min and cooled down by immediately transferring the sample holder to a

L. F. Zagonel, R. L. O. Basso, F. Alvarez
Instituto de Física "Gleb Wataghin", Universidade Estadual de
Campinas, Unicamp, P.O. Box 6165, Campinas, SP 13083-970,
Brazil
E-mail: lzagonel@cea.br

Table 1. AISI H13 steel composition, atomic percent.

Element	Fe	C	Mn	Si	Cr	Mo	V
Content (± 0.1)	87.3	2.5	0.4	2.1	5.9	0.8	1

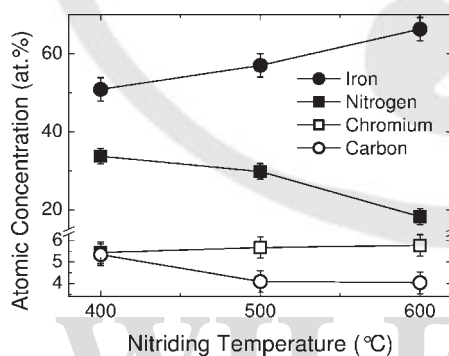
massive support at room temperature. The XPS studies were performed with a VG-CLAM-2 electron energy analyzer and a non-monochromatic $AlK\alpha$ X-ray source. The total apparatus resolution (analyzer plus line-width) is ~ 0.8 eV. The information regarding the crystalline structure was gathered in the Bragg-Brentano X-ray diffraction (XRD) geometry using monochromatized $CuK\alpha_1$ radiation. Surface sputtered depth and surface roughness were determined by means of profilometry.

In order to study the nitrided layer, the samples were sectioned transversally. Then, the exposed cross-sections were covered by a protective electroplated nickel layer and polished (last step $0.25 \mu\text{m}$) for electron probe microanalysis (EPMA) and scanning electron microscopy (SEM) investigations without etching. EPMA was performed employing a Cameca SX100 at Max Planck Institute for Metals Research (Stuttgart, Germany) while SEM employed a Jeol JMS-5900LV at the Laboratório Nacional de Luz Síncrotron (Campinas, Brazil). For the EPMA, a 10 kV focused electron beam of 100 nA was applied. To obtain the element concentration, the characteristic X-ray intensity of each element was determined and divided by the intensity obtained from standards (pure metals, Fe_3C , and Fe_4N , for iron and alloys, carbon, and nitrogen, respectively). The needed corrections were calculated applying the $\Phi(\rho z)$ method, according to the procedure found in ref.^[8] The SEM images were recorded with 10 kV electron by using the backscattered electron signal from a solid-state detector.

Results and Discussion

X-Ray Photoelectron Spectroscopy

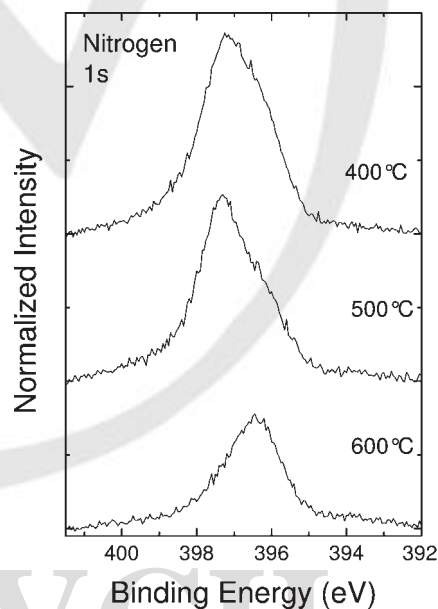
XPS is able to provide precise information on the sample surface composition (~ 1 nm, for $AlK\alpha$ X-ray) immediately after the nitriding process.^[9] Figure 1 shows the results for samples prepared at different temperatures. It is observed

**Figure 1.** Surface concentration of major H13 steel elements after nitriding at different temperatures.

that at 400°C the nitrogen concentration is the highest obtained, decreasing with increasing temperatures.

We note that the nitrogen ion flux on the sample surface is constant. It only depends on the (constant) ion current from the ion gun. Considering that the nitrogen chemical reaction on the surfaces is relatively fast for all the studied samples, increasing nitrogen diffusion into the bulk material on increasing the temperature is expected, i.e., the surface is nitrogen depleted by augmenting the nitriding temperature. In other words, the competition between the arriving nitrogen flux and the diffusion flux determines the nitrogen concentration at the surface samples. We remark that this is an interesting difference from the gas nitriding process where the nitrogen chemical potential is a temperature-dependent variable derived from the thermodynamic equilibrium of the system.^[10] As displayed in Figure 1, decarburizing and a small increase in chromium concentration at 500°C and 600°C were also observed.

The analysis of the core level electrons by XPS provides valuable information on the elemental chemical states. In particular, the N1s peaks show a dependence on the process temperature, a fingerprint of different chemical bonds (Figure 2). At 400°C , a broad peak is observed stemming from nitrogen bonds to iron and alloying material elements. At 500°C , some contributions disappear and a more asymmetric core level, shifted to higher binding energies, is observed. Differently, at 600°C , the peak is narrower, shifted to lower energies. The EPMA and XRD results were used to identify the compounds as chromium nitride CrN (-396.5 eV) and iron nitride Fe_3N (-397.4 eV)

**Figure 2.** XPS peaks associated to N1s electron core levels for samples nitrided at different temperatures.

for the 600 and 500 °C samples, respectively, in agreement with the literature results.^[11,12] Indeed, the broad peak observed for 400 and 500 °C indicate that, both chromium and iron nitrides are formed on these temperatures, while at 600 °C nitrogen is mostly as chromium nitride. The peak associated with the Cr2p^{3/2} electron core level (not shown) also displays an energy shift, from -565.1 eV (untreated sample) to -566.4 eV (600 °C), also in agreement with literature values for metallic chromium and CrN.^[11,12] This indicates that the formation of chromium nitrides is more favorable at higher temperatures, regardless of the nitrogen concentration.

EPMA

Figure 3 displays nitrogen profiles measured by EPMA line scans.^[13] Each point corresponds to a $\sim 1 \mu\text{m}^3$ excitation volume. As observed, at 400 °C the diffusion profile is smooth and follows a complementary error function (erfc).^[14] The erfc fit to the curve in Figure 3 is the solution of Fick's Law for a constant surface concentration boundary condition and determines an effective diffusion coefficient of $1.0 \times 10^{-14} \text{ m}^2 \cdot \text{s}^{-1}$. At 500 °C the profile shows deviations from the erfc behavior and a thin nitrogen rich layer is observed on top. On the contrary, higher temperatures induce the formation of an extended step-like nitrogen profile presenting two characteristics: (a) relatively low nitrogen concentration and (b) a abundant nitrogen precipitates (each peak in the nitrogen profile has an associated peak in an alloying element profile). The relative low surface nitrogen concentration agrees with the XPS results, indicating that, even at constant nitrogen flux, i.e., constant ion beam current density, the surface concentration depends on the bulk nitrogen diffusion coefficients. Therefore, appropriated

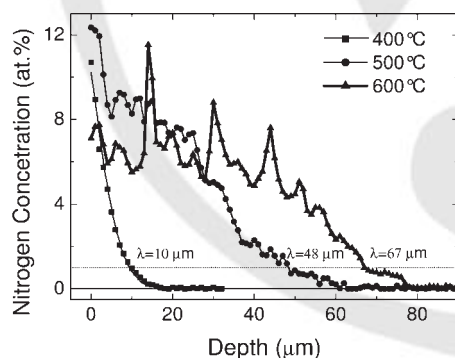


Figure 3. Nitrogen profile measured by EPMA line scans for samples nitrided at different temperatures. The lines are a guide to the eyes for 500 and 600 °C and an erfc for 400 °C. The characteristic temperature-dependent nitrogen penetration depth, λ , is estimated by drawing a horizontal line at 1 at.-% nitrogen concentration.

boundary conditions at the surface should be applied when solving diffusion equations. In addition, the nitriding regime seems to change from low to high temperatures following diffusion and internal oxidation models, respectively.^[15–17]

The surface nitrogen concentration is affected not only by nitrogen diffusion and by the incident nitrogen flux but also, in the case of ion beam nitriding, by other ion interactions with matter such as sputtering. This process is responsible for the removal of material from the sample surface, and it is beneficial in removing oxide layers that prevent an adequate nitrogen concentration at the material surface. In the present study, the observed depths due to sputtering are smaller than $1 \mu\text{m}$ for all the studied samples and, therefore, have negligible effect on the total nitrided depth. However, especially with high nitrogen surface concentration, desorption of nitrogen can be important.

The component concentration profiles obtained by EPMA line scan are shown for the sample nitrided at 500 °C (Figure 4). The unnitrided core is shown on the right-hand side where it is possible to distinguish, following the concentration lines, some chromium carbide precipitates which can be observed as well by SEM and are characteristic of the H13 steel. Upon nitriding at such temperature, the chromium carbide compounds seem to be dissolved. Therefore, the free carbon migrates forming vanadium carbides (Figure 4). Apparently, chromium forms submicrometric nitride precipitates that could not be clearly distinguished in SEM images, creating a smoother profile near the surface. This is an intermediate behavior occurring at temperatures between 400 °C, in which precipitates may be only nanometric, and at 600 °C, in which large precipitates are observed. Indeed, the profile of chromium in the sample nitrided at 600 °C, i.e., segregates, accompanies nitrogen profile (Figure 3).

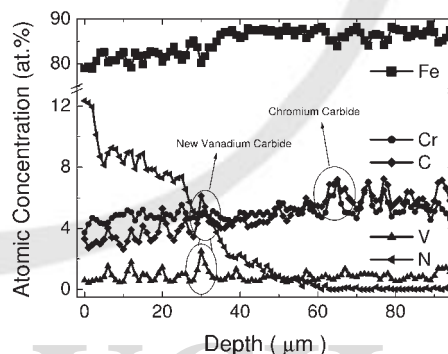


Figure 4. Concentration profile of major steel component elements for the sample nitrided at 500 °C. Among the precipitates within the profile, two are assigned.

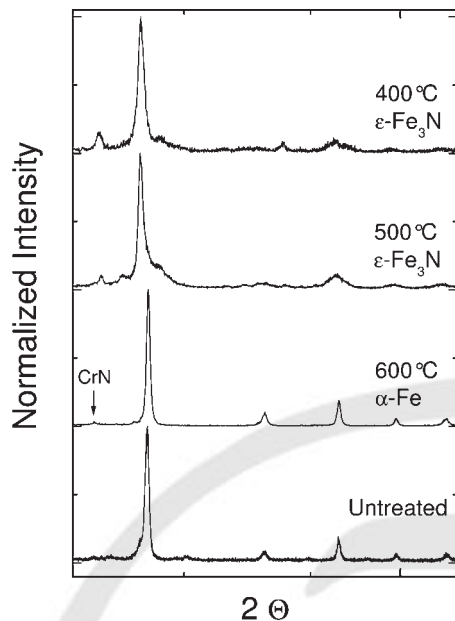


Figure 5. XRD diffractograms from samples nitrided at different temperatures. The results from an untreated sample are also displayed. The relevant peaks are related to the assigned phases.

X-Ray Diffraction

Figure 5 displays the diffraction patterns obtained from the nitrided samples. For comparison purposes, the diffractogram of a pristine material is also displayed. As observed, at 400 and 500 °C, the ϵ -Fe₃N phase is sizable at the material surface, suggesting that precipitates are not preferentially formed. At 600 °C, on the contrary, the α -Fe present in the pristine material is preserved. This observation suggests that the relative small amount of nitrogen at such high temperatures forms precipitates preferentially than FeN_x compounds. The main precipitate formed is CrN which could be resolved by XRD and XPS and observed on SEM images (Figure 6). The crystalline phases observed at the surfaces closely coincide with the concentration and chemical states determined by XPS. The same is valid for the concentration of nitrogen and nitride precipitate formation, as determined by EPMA. Finally, we note that the peak width also indicates that at higher temperatures the stress and/or composition gradients are much smaller, as expected if one considers that the steel grain size, about 10 μ m, does not change during the nitriding process, as determined by SEM.

SEM

Figure 6 shows an SEM image in backscattered electron mode indicating that the precipitates in the first 40 μ m of the nitrided zone have larger size and density, in

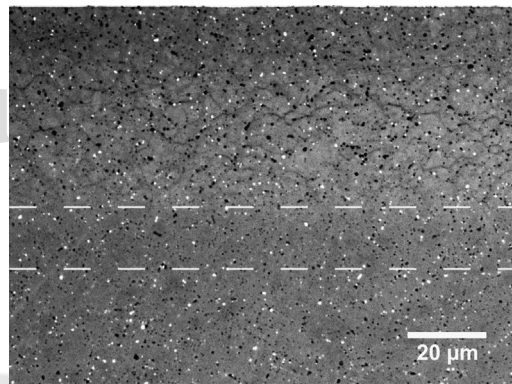


Figure 6. Micrograph obtained from the sample nitrided at 600 °C showing precipitates (white and black dots) near to the material surface. The horizontal lines mark the depths with nitrogen concentration of 4 and 1 at.-%, from top to bottom.

agreement with EPMA profiles. This result was, indeed, confirmed by obtaining images with higher magnification (not shown). The observed dark spots and white spots correspond to chromium or vanadium precipitates and molybdenum precipitates, respectively, as determined by EDS and EPMA.^[18] Figure 6 also displays some distinguishable dark elongated structures which resemble grain boundaries. This pattern is similar to the grain structure observed on untreated samples and chemically etched to reveal their morphology.

Conclusion

In spite of constant nitrogen ion current density, the temperature dependence of the diffusion process causes different surface nitrogen concentrations. Moreover, different nitrogen profiles and precipitates are obtained in the nitrided material. At 500 and 600 °C, nitriding causes decarburization at the surface with vanadium carbide formation due to carbon stemming from chromium carbide dissolution. Also at 600 °C, the smaller nitrogen concentration stabilizes the ferrite phase throughout the nitriding process. Below such temperature, iron nitrides are formed with the accumulation of nitrogen at the surface. Finally, the precipitation of chromium and iron nitrides seems to be a competitive process. The higher nitrogen affinity for chromium leads to the formation of CrN compounds provided that the temperature is high enough to allow the dissolution of its carbides and subsequent diffusion of chromium.

Acknowledgements: We are grateful to Professor E. J. Mittemeijer and Mrs. S. Haug from Max-Planck-Institute for Metals Research for an insightful discussion and for assistance with the electron

probe microanalysis measurements, respectively. This work was partially supported for FAPESP, project 97/12069-0. L. F. Z. is FAPESP and DAAD fellow. F. A. is CNPQ [fellow](#)^{Q1}.

Received: September 8, 2006; Revised: December 1, 2006;
Accepted: December 6, 2006; DOI: 10.1002/ppap.200731808

Keywords: diffusion; ion implantation; nitrides; plasma nitriding; precipitates

- [1] M. A. Pessin, M. D. Tier, T. R. Strohaecker, A. Bloyce, Y. Sun, T. Bell, *Tribol. Lett.* **2000**, *8*, 223.
- [2] M. Uma Devi, T. K. Chakraborty, O. N. Mohanty, *Surf. Coat. Technol.* **1999**, *116*, 212.
- [3] T. Bell, Y. Sun, Q. Suhadi, *Vacuum* **2000**, *59*, 14.
- [4] S. R. Kasi, H. Kang, C. S. Sass, J. W. Rabalais, *Surf. Sci. Rep.* **1989**, *10*, 1.
- [5] T. Czerwicz, H. Michel, E. Bergmann, *Surf. Coat. Technol.* **1998**, *108*, 182.
- [6] H. R. Kaufman, J. J. Cuomo, J. M. E Harper, *J. Vac. Sci. Technol.* **1982**, *21*, 725.
- [7] P. Hammer, N. M. Victoria, F. Alvarez, *J. Vac. Sci. Technol. A* **1998**, *16*, 2941.
- [8] J. L. Pouchou, F. Pichoir, *Rech. Aerosp.* **1984**, *3*, 167.
- [9] W. S. M. Werner, *Surf. Interface Anal.* **2001**, *31*, 141.
- [10] E. J. Mittemeijer, J. T. Slycke, *Surf. Eng.* **1996**, *12*, 152.
- [11] P. C. J. Graat, M. A. J. Somers, E. J. Mittemeijer, *Appl. Surf. Sci.* **1998**, *136*, 238.
- [12] A. Lippitz, Th. H. übert, *Surf. Coat. Technol.* **2005**, *200*, 250.
- [13] G. A. Collins, R. Hutching, J. Tendys, *Surf. Coat. Technol.* **1993**, *59*, 267.
- [14] M. Ueda, C. Leandro, H. Reuther, C. M. Lepienski, *Nucl. Instrum. Methods Phys. Res. B* **2005**, *240*, 204.
- [15] R. E. Schacherl, P. C. J. Graat, E. J. Mittemeijer, *Metall. Mater. Trans. A*, **2004**, *35*, 3387.
- [16] M. Gouné, T. Belmonte, J. M. Fiorani, S. Chomer, H. Michel, *Thin Solid Films* **2000**, *337*, 543.
- [17] Y. Sun, T. Bell, *Mater. Sci. Eng. A* **1997**, *224*, 33.
- [18] L. F. Zagonel, C. A. Figueroa, F. Alvarez, *Surf. Coat. Technol.* **2005**, *200*, 2566.

Q1: Please clarify whether LKS and FA are recipients of fellowships from FAPSEP and CNPQ, respectively.

WILEY-VCH